

Pair-instability mass loss for top-down compact object mass calculations

M. RENZO,^{1,2} D. D. HENDRIKS,³ L. A. C. VAN SON,^{4,5,6} AND R. FARMER⁶

¹*Center for Computational Astrophysics, Flatiron Institute, New York, NY 10010, USA*

²*Department of Physics, Columbia University, New York, NY 10027, USA*

³*Department of Physics, University of Surrey, Guildford, GU2 7XH, Surrey, UK*

⁴*Center for Astrophysics | Harvard & Smithsonian, 60 Garden St., Cambridge, MA 02138, USA*

⁵*Anton Pannekoek Institute for Astronomy, University of Amsterdam, Science Park 904, 1098XH Amsterdam, The Netherlands*

⁶*Max-Planck-Institut für Astrophysik, Karl-Schwarzschild-Straße 1, 85741 Garching, Germany*

ABSTRACT

Population synthesis relies on semi-analytic formulae to determine masses of compact objects from the (helium or carbon-oxygen) cores of collapsing stars. Such formulae are combined across mass ranges that span different explosion mechanisms, potentially introducing artificial features in the compact object mass distribution. Such artifacts impair the interpretation of gravitational-wave observations. We propose a “top-down” remnant mass prescription where we remove mass from the star for each possible mass-loss mechanism, instead of relying on the fallback onto a “proto-compact-object” to get the final mass. For one of these mass-loss mechanisms, we fit the metallicity-dependent mass lost to pulsational-pair instability supernovae from numerical simulations. By imposing no mass loss in the absence of pulses, our approach recovers the existing compact object masses at the low mass end and ensures continuity across the core-collapse/pulsational-pair-instability regime.



1. INTRODUCTION

Stellar and binary population synthesis calculations are necessary to predict event rates and population statistics of astrophysical phenomena, including those involving neutron stars (NS) and black holes (BH). Typically, at the end of the evolution (carbon depletion) the mass of the core is mapped to a compact object mass, using a $M_{\text{comp. obj}} \equiv M_{\text{comp. obj}}(M_{\text{core}})$ informed by core-collapse (CC) simulations (e.g., Fryer et al. 2012; Spera et al. 2015; Mandel & Müller 2020; Couch et al. 2020, see also Zapartas et al. 2021; Patton et al. 2021) and/or (pulsational) pair instability (PPI) simulations (e.g., Belczynski et al. 2016; Woosley 2017; Spera & Mapelli 2017; Stevenson et al. 2019; Marchant et al. 2019; Farmer et al. 2019; Breivik et al. 2020; Renzo et al. 2020b; Costa et al. 2021).

The most commonly adopted algorithms to obtain compact object masses in the CC regime are the “rapid” and “delayed” prescriptions of Fryer et al. (2012). In both cases, the compact object is built from the “bottom-up”, starting from a proto-NS mass and adding the amount of fallback expected in the (possibly failed) explosion. However, the proto-NS mass and information about the core structure relevant to calculate the fall-

back are usually not available (e.g., Patton & Sukhbold 2020). Instead, the total final mass of the star is arguably easier to constrain in population synthesis models.

At the transition between CC and PPI (roughly at carbon-oxygen cores of $\sim 35 M_{\odot}$, Woosley 2017; Marchant et al. 2019; Farmer et al. 2019; Renzo et al. 2020b; Costa et al. 2021), a mismatch between commonly adopted fitting formulae exists, and impairs the interpretation of gravitational-wave data (as pointed out in Fig. 5 of van Son et al. 2021). While it is possible that the BH mass function is discontinuous at the onset of the PPI regime (e.g., Renzo et al. 2020c; Costa et al. 2021, Hendriks et al., in prep.), the location and amplitude of a putative discontinuity should not be governed by a mismatch between the fitting formulae.

2. TOP-DOWN COMPACT OBJECT MASSES

In contrast with the “bottom up” approach of Fryer et al. (2012), we propose a “top-down” compact object mass calculation. Starting from the total stellar mass, we remove the amount of mass lost due to all of the processes associated with the (possibly failed) explosion:

$$M_{\text{comp. obj}} = M_{\text{pre-CC}} - (\Delta M_{\text{SN}} + \Delta M_{\nu,\text{core}} + \Delta M_{\text{env}} + \Delta M_{\text{PPI}} + \dots) \quad (1)$$

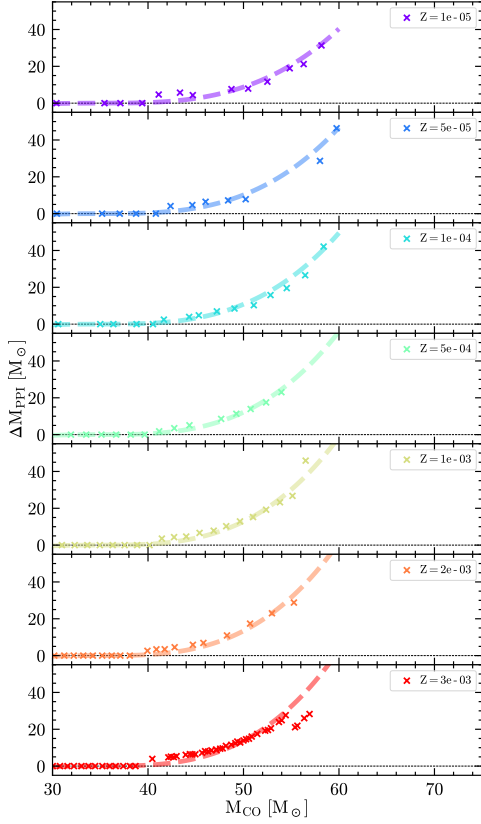


Figure 1. Each panel shows our fitting formula Eq. 2 for the PPI induced mass-loss as a function of carbon-oxygen core mass at each metallicity Z . The crosses show the values from Tab. 1 Farmer et al. (2019).

where $M_{\text{pre-CC}}$ is the total mass at the onset of CC, and each term in parenthesis corresponds to a potential mass-loss mechanism: ΔM_{SN} for the CC ejecta, $\Delta M_{\nu,\text{core}}$ the change in gravitational mass of the core due to the neutrino losses, ΔM_{env} the loss of the envelope that can occur even in red supergiant “failed” core-collapse due to $\Delta M_{\nu,\text{core}}$ (Nadezhin 1980; Lovegrove &

Woosley 2013; Piro 2013; Fernández et al. 2018; Ivanov & Fernández 2021), and ΔM_{PPI} the pulsational mass loss due to pair-instability. Each term may be a function of the progenitor properties, and may be theoretically or observationally informed (e.g., ΔM_{SN} could be derived from the light curves of a large sample of observed SNe). Eq. 1 can be extended by adding additional mass-loss mechanisms in the parenthesis (e.g., disk winds).

In the CC regime, the previous approach from Fryer et al. (2012) can be recovered by setting $\Delta M_{\text{SN}} + \Delta M_{\nu,\text{core}} = M_{\text{pre-CC}} - M_{\text{comp. obj}}^{\text{Fryer+12}}$, where the last term is the compact object mass as predicted by Fryer et al. (2012) and ignoring the other mass loss terms, such as ΔM_{PPI} and ΔM_{env} .

3. NEW FIT FOR PPI EJECTA

Imposing $\Delta M_{\text{PPI}} = 0$ at the edge of the PPI regime, Eq. 1 produces a smooth BH mass distribution. Eq. 2 provides a fit (in M_{\odot} units) to naked helium star models from Farmer et al. (2019) for $\Delta M_{\text{PPI}} \equiv \Delta M_{\text{PPI}}(M_{\text{CO}}, Z)$. While the fit of Farmer et al. (2019) provides the BH mass after PPI, this is only an estimate because of other mass loss processes that might occur at CC (e.g., Renzo et al. 2020b; Powell et al. 2021; Rahman et al. 2021). Here, we fit the mass removed by PPI (crosses in Fig. 1), which is what is directly computed in Farmer et al. (2019).

We neglect the (weak) metallicity dependence of the minimum core mass for PPI, and we fit the data for initial helium core masses between $38 - 60 M_{\odot}$. We emphasize that Farmer et al. (2019) only simulated helium cores. In the presence of a H-rich envelope at the onset of PPI, if it is extended and red it can be easily removed by the first pulse (Woosley 2017; Renzo et al. 2020b). Thus the H-rich mass of red supergiants should be added to the ΔM_{PPI} provided here. It is unclear what occurs in cases when the envelope is compact and blue (e.g., Di Carlo et al. 2019; Renzo et al. 2020a; Costa et al. 2021).

$$\Delta M_{\text{PPI}} = (0.0006 \log_{10}(Z) + 0.0054) \times (M_{\text{CO}} - 34.8)^3 - 0.0013 \times (M_{\text{CO}} - 34.8)^2 \quad (2)$$

The mass lost in PPI is sensitive to convection (Renzo et al. 2020c) and nuclear physics (Farmer et al. 2019,

2020; Costa et al. 2021; Woosley & Heger 2021; Mehta et al. 2021), which can introduce uncertainties up to $\sim 20\%$ on the maximum BH mass. The accuracy of our fit is comparable to these uncertainties.

REFERENCES

Belczynski, K., Heger, A., Gladysz, W., et al. 2016, A&A,

594, A97, doi: 10.1051/0004-6361/201628980

Breivik, K., Coughlin, S., Zevin, M., et al. 2020, ApJ, 898,

71, doi: 10.3847/1538-4357/ab9d85

- Costa, G., Bressan, A., Mapelli, M., et al. 2021, MNRAS, 501, 4514, doi: [10.1093/mnras/staa3916](https://doi.org/10.1093/mnras/staa3916)
- Couch, S. M., Warren, M. L., & O'Connor, E. P. 2020, ApJ, 890, 127, doi: [10.3847/1538-4357/ab609e](https://doi.org/10.3847/1538-4357/ab609e)
- Di Carlo, U. N., Giacobbo, N., Mapelli, M., et al. 2019, MNRAS, 487, 2947, doi: [10.1093/mnras/stz1453](https://doi.org/10.1093/mnras/stz1453)
- Farmer, R., Renzo, M., de Mink, S. E., Fishbach, M., & Justham, S. 2020, ApJL, 902, L36, doi: [10.3847/2041-8213/abbadd](https://doi.org/10.3847/2041-8213/abbadd)
- Farmer, R., Renzo, M., de Mink, S. E., Marchant, P., & Justham, S. 2019, ApJ, 887, 53, doi: [10.3847/1538-4357/ab518b](https://doi.org/10.3847/1538-4357/ab518b)
- Fernández, R., Quataert, E., Kashiyama, K., & Coughlin, E. R. 2018, MNRAS, 476, 2366, doi: [10.1093/mnras/sty306](https://doi.org/10.1093/mnras/sty306)
- Fryer, C. L., Belczynski, K., Wiktorowicz, G., et al. 2012, ApJ, 749, 91, doi: [10.1088/0004-637X/749/1/91](https://doi.org/10.1088/0004-637X/749/1/91)
- Ivanov, M., & Fernández, R. 2021, ApJ, 911, 6, doi: [10.3847/1538-4357/abe59e](https://doi.org/10.3847/1538-4357/abe59e)
- Lovegrove, E., & Woosley, S. E. 2013, ApJ, 769, 109, doi: [10.1088/0004-637X/769/2/109](https://doi.org/10.1088/0004-637X/769/2/109)
- Mandel, I., & Müller, B. 2020, MNRAS, 499, 3214, doi: [10.1093/mnras/staa3043](https://doi.org/10.1093/mnras/staa3043)
- Marchant, P., Renzo, M., Farmer, R., et al. 2019, ApJ, 882, 36, doi: [10.3847/1538-4357/ab3426](https://doi.org/10.3847/1538-4357/ab3426)
- Mehta, A. K., Buonanno, A., Gair, J., et al. 2021, arXiv:2105.06366. <https://arxiv.org/abs/2105.06366>
- Nadezhin, D. K. 1980, Ap&SS, 69, 115, doi: [10.1007/BF00638971](https://doi.org/10.1007/BF00638971)
- Patton, R. A., & Sukhbold, T. 2020, MNRAS, 499, 2803, doi: [10.1093/mnras/staa3029](https://doi.org/10.1093/mnras/staa3029)
- Patton, R. A., Sukhbold, T., & Eldridge, J. J. 2021, arXiv:2106.05978. <https://arxiv.org/abs/2106.05978>
- Piro, A. L. 2013, ApJL, 768, L14, doi: [10.1088/2041-8205/768/1/L14](https://doi.org/10.1088/2041-8205/768/1/L14)
- Powell, J., Müller, B., & Heger, A. 2021, MNRAS, 503, 2108, doi: [10.1093/mnras/stab614](https://doi.org/10.1093/mnras/stab614)
- Rahman, N., Janka, H.-T., Stockinger, G., & Woosley, S. 2021, arXiv:2112.09707. <https://arxiv.org/abs/2112.09707>
- Renzo, M., Cantiello, M., Metzger, B. D., & Jiang, Y. F. 2020a, ApJL, 904, L13, doi: [10.3847/2041-8213/abc6a6](https://doi.org/10.3847/2041-8213/abc6a6)
- Renzo, M., Farmer, R., Justham, S., et al. 2020b, A&A, 640, A56, doi: [10.1051/0004-6361/202037710](https://doi.org/10.1051/0004-6361/202037710)
- Renzo, M., Farmer, R. J., Justham, S., et al. 2020c, MNRAS, 493, 4333, doi: [10.1093/mnras/staa549](https://doi.org/10.1093/mnras/staa549)
- Spera, M., & Mapelli, M. 2017, MNRAS, 470, 4739, doi: [10.1093/mnras/stx1576](https://doi.org/10.1093/mnras/stx1576)
- Spera, M., Mapelli, M., & Bressan, A. 2015, MNRAS, 451, 4086, doi: [10.1093/mnras/stv1161](https://doi.org/10.1093/mnras/stv1161)
- Stevenson, S., Sampson, M., Powell, J., et al. 2019, ApJ, 882, 121, doi: [10.3847/1538-4357/ab3981](https://doi.org/10.3847/1538-4357/ab3981)
- van Son, L. A. C., de Mink, S. E., Callister, T., et al. 2021, arXiv:2110.01634. <https://arxiv.org/abs/2110.01634>
- Woosley, S. E. 2017, ApJ, 836, 244, doi: [10.3847/1538-4357/836/2/244](https://doi.org/10.3847/1538-4357/836/2/244)
- Woosley, S. E., & Heger, A. 2021, ApJL, 912, L31, doi: [10.3847/2041-8213/abf2c4](https://doi.org/10.3847/2041-8213/abf2c4)
- Zapartas, E., Renzo, M., Fragos, T., et al. 2021, arXiv:2106.05228. <https://arxiv.org/abs/2106.05228>